

Ultrafast laser-induced order-disorder transitions in semiconductors

K. Sokolowski-Tinten, J. Bialkowski, and D. von der Linde

Institut für Laser- und Plasmaphysik, Universität-GHS-Essen, D-45117 Essen, Federal Republic of Germany

(Received 16 January 1995)

Laser-induced ultrafast order-disorder transitions in silicon and gallium arsenide are studied by means of femtosecond time-resolved linear and nonlinear optical spectroscopy. Detailed measurements of the reflectivity and of the reflected second harmonic over a wide range of fluences reveal a complex picture of the phase transformation. We show that during the first 100 fs the changes of the optical constants and of the nonlinear optical susceptibility $\chi^{(2)}$ are determined by the various electronic excitation processes and only to a lesser extent by the process of disordering. On the other hand, time-resolved measurements of reflectivity spectra indicate that the development of a Drude-like metallic spectrum takes a few hundred femtoseconds. Our data show that the laser-induced structural changes develop slower than previously believed, occurring on a time scale of a few hundred femtoseconds.

I. INTRODUCTION

Laser-induced phase transitions in materials such as silicon, germanium, and gallium arsenide have been the subject of a great number of investigations ever since the discovery of laser annealing¹ of crystal damage in ion-implanted semiconductors. Both the technological aspects of laser processing² and the fundamental physics issues³ have been studied extensively.

This paper deals with laser-induced solid-to-liquid transitions. When the time scale of these processes is much longer than the thermalization time of the absorbed optical energy, which is typically of the order of 1 ps, the physics of these transformations is quite well understood. It is generally accepted⁴ that in this case the transitions can be explained in terms of thermal processes. Thus, even for pulses as short as a few tens of picoseconds, a thermal model is usually adequate.

On the other hand, the situation is different when much shorter laser pulses are used. Studies of laser-induced phase transformations using femtosecond laser pulses have revealed ultrafast transformations that occur on a subpicosecond time scale, faster than the relaxation of the optical energy. For example, Shank *et al.*⁵ performed time-resolved measurements of the optical reflectivity of femtosecond laser-excited silicon and concluded that the transformation of the covalent solid material to the metallic liquid phase can take place in less than 1 ps. Similar results have been obtained in gallium arsenide,⁶⁻⁹ graphite,^{10,11} and diamond.^{11,12}

The observation of reflectivity changes consistent with an ultrafast melting process have been supported by measurements of the reflected second harmonic (SH).^{6-9,13,14} Surface second-harmonic generation can provide, in principle, information about the structural symmetry of the material¹⁵ because the nonlinear susceptibility tensor reflects the symmetry of the crystal lattice. The rapid changes of the SH observed in silicon and gallium arsenide after femtosecond laser excitation have been in-

terpreted as evidence of changes or loss of crystalline symmetry.

Several attempts have been made¹⁶⁻²² to explain the ultrafast phase transformations in terms of a carrier-induced softening of the crystal lattice,^{23,24} invoking the so-called plasma model of laser annealing.¹⁶ However, a complete understanding of the mechanisms leading to ultrafast disordering is still lacking.

We have shown in a recent study⁸ that in femtosecond laser-excited gallium arsenide two different types of phase transformations can be observed. For laser fluences up to about 1.5 times the threshold fluence a slow transformation very similar to thermal melting induced by picosecond pulses (or longer) is observed. On the other hand, for fluences greater than two times the threshold the ultrafast transformation takes over.

One of the main problems in studying laser-induced solid-liquid transitions by optical techniques is to distinguish the highly excited solid from the final metallic liquid. With femtosecond laser excitation the density of electron-hole pairs is of the order of $N_{e-h} \approx 10^{22} \text{ cm}^{-3}$. The properties of such an extremely dense electron-hole plasma are qualitatively similar to the properties of a simple metal. It has been realized^{7-9,14} that changes of reflectivity and SH resulting from a structural transition may be obscured by the laser-induced changes of the linear and the nonlinear optical properties due to the dense free-carrier plasma and also by changes of the population of the valence and the conduction band. Here we present more detailed experimental data on femtosecond time-resolved measurements of the optical reflectivity and the reflected second harmonic. Particular emphasis is placed on the distinction between the initial excitation stage of the intact solid structure and the proper transition stage in which the structural changes develop.

The paper is organized as follows. Section II gives a brief description of the experimental methods. In Sec. III the results of our time-resolved experiments are presented. Section IV gives a detailed analysis of the exper-

imental results. We extract from our data the complex index of refraction and the nonlinear optical susceptibility, which describe the linear and the nonlinear optical properties of the excited material as a function of time. In Sec. V we discuss the observed changes of the optical properties in terms of the underlying physical processes and try to identify the mechanisms leading to ultrafast disordering.

II. EXPERIMENT

To study the laser-induced phase transition detailed measurements of the *s*- and the *p*-polarized reflectivity (silicon and gallium arsenide) and of the reflected second harmonic (only gallium arsenide) were performed. These single wavelength measurements allowed us to precisely monitor the temporal evolution of the different processes accompanying the laser-induced phase transition. In addition, time-resolved measurements of the spectra of the optical reflectivity over a wide range of wavelengths were carried out, which permitted us to clearly identify the liquid state.

We applied standard femtosecond pump-probe techniques. Femtosecond laser pulses derived from a colliding pulse, passively mode-locked dye laser (rhodamine 6G/DODCI) were amplified at a repetition rate of 10 Hz. The amplifier consisted of a six-pass preamplifier and two final amplifier stages (axicon and Bethune cells).²⁵ A maximum output energy of a few millijoule at 625 nm was obtained and the pulse duration was between 60 and 100 fs, depending on the fine tuning of the laser system. The samples were single-crystalline, optically polished, undoped wafers of silicon and gallium arsenide with (100)- or (111)-surface orientation. No dependence of the melting behavior on crystal orientation could be observed. The wafers were raster scanned during the experiments, using a x-y-translation stage driven by a stepper motor. In this way a fresh, unexcited surface was provided for each laser pulse.

The probe pulses for measuring the reflectivity and the reflected SH were derived from the pump pulses by splitting off a small fraction from the pump. The pump beam struck the sample surface at an angle of incidence of 56° . The probe beam was focused down to the central 5% of the pumped area at an angle of incidence of 70.5° . We measured simultaneously both the *s*- and the *p*-polarized component of the reflected probe pulse. Note that the angle of incidence of the probe beam is close to the principal angle of incidence, where the *p*-polarized reflectivity runs through a minimum. For this choice of the angle the laser-induced relative changes of the *p* component of the reflectivity are quite strong.^{26,27}

The fluence of the probe pulse was kept at a level of about a few hundred $\mu\text{J}/\text{cm}^2$, well below the single-exposure melting threshold at 625 nm. It was also low enough to prevent undesired heating when, after melting, the probe pulse interacted with the very strongly absorbing liquid surface ($\alpha_{\text{liq}} \approx 10^6 \text{ cm}^{-1}$).^{8,28} In gallium arsenide, which possesses a strong nonlinear optical susceptibility $\chi^{(2)}$, we also measured the *s*-polarized SH in

addition to the optical reflectivity. In the SH experiments the gallium arsenide sample was oriented with the (001) crystal axis perpendicular to the plane of incidence. In this configuration SH generation of the much stronger *s*-polarized pump beam is suppressed because it is symmetry forbidden, whereas the *s*-polarized SH of the *p*-polarized probe beam is allowed. Coherent coupling effects between pump and probe pulses were avoided by using perpendicular polarizations for pump and probe.

For the observation and control of the spatial beam profile a diode array was used to monitor the intensity distribution of the pump beam in a reference plane representing a replica of the target surface. This configuration permitted measurements of the local pump fluence on the area actually interrogated by the probe pulse, in addition to the measurement of the total incident pump energy. Because small pulse-to-pulse variations in the beam profile of the amplified pulse could not be completely avoided, the local pump fluence turned out to be a much better energy reference than the total pump energy. By using this method of monitoring the pump laser fluence, the scattering of the measured reflectivity and the SH data could be greatly reduced.

The spectra of the optical reflectivity were measured using a white light femtosecond continuum²⁹ as a probe. The continuum was generated in a 5-mm-long piece of fused silica and extended from 380 nm to approximately 850 nm. After spatial filtering the white light was focused onto the center of the excited area. To avoid chromatic aberrations, an aluminum-coated mirror was used for focusing. The spectra were recorded by a flat-field spectrograph in conjunction with a cooled, computer-controlled charge coupled device detector. The angles of incidence for the pump and the probe beam were 0° and 11° , respectively, and the polarizations were perpendicular. The continuum probe pulses acquired some temporal delay of ≈ 5 ps between the far red and far blue component, due to the group-velocity dispersion of the various optical components. As a consequence, there was a spread of delay times across the recorded raw spectra. To extract spectra with the full femtosecond time resolution a deconvolution procedure was applied to the whole set of spectra representing the different optical delays. By measuring the cross correlation between selected spectral portions of the continuum and the pump pulse we verified that a time resolution of about 100 fs was indeed maintained.

III. EXPERIMENTAL RESULTS

Figure 1 presents an overview of the typical behavior of the reflected SH (upper panel) and the *s*- and the *p*-polarized optical reflectivity (lower panel) for gallium arsenide during the first picosecond after excitation. The pump fluence in this example was two times the melting threshold, which has been measured to be $F_m = 170 \text{ mJ}/\text{cm}^2$ for gallium arsenide under the conditions of our experiment.

At a first glance the observed time dependence appears to be consistent with the expected behavior of a

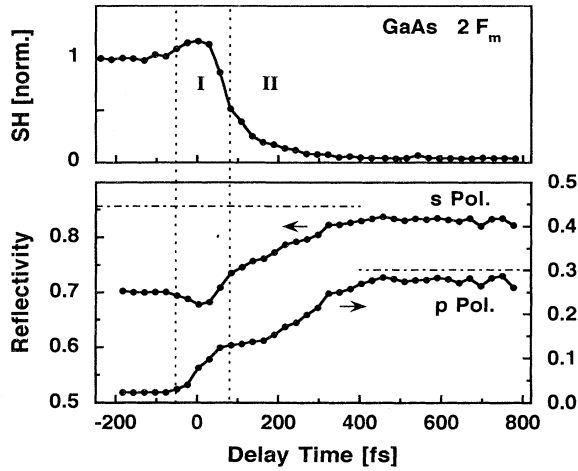


FIG. 1. Measured *s*- and *p*-polarized reflectivity and reflected SH of gallium arsenide ($\lambda = 625$ nm, $\Theta_{in} = 70^\circ$) as a function of delay time. The pump fluence is 0.34 J/cm² ($\approx 2F_m$). The different stages of signal evolution are marked by the dashed lines. The dash-dotted lines mark the reflectivities of liquid gallium arsenide.

solid-liquid phase transformation: an increase of the reflectivity and a drop of the SH intensity accompanying the transition from the covalent, non-centrosymmetric solid phase to the metallic, centrosymmetric liquid phase. However, a closer inspection of the data reveals a more complicated structure of the time evolution. Two distinct stages of the transformation, denoted I and II, can be distinguished. These are marked in Fig. 1 by dashed lines. Stage I corresponds to the first 100 fs, when the pump pulse is still present. Inspection of the SH signal during stage I shows an initial slight increase preceding the rapid decrease. Comparing reflectivity and the SH we find that the behavior of the *s*-polarized optical reflectivity is somewhat similar to the SH with the opposite sign: there is a slight decrease first, followed by an increase. The *p*-polarized reflectivity, on the other hand, increases monotonously during stage I. There is some significant slowing down in the evolution of both reflectivity and SH after the end of the pump pulse. The SH signal drops down to a very low level in about 200 fs, while the reflectivities exhibit a relatively slow further increase. Finally, the SH disappears completely and the reflectivities approach values corresponding to the metallic liquid phase (dash-dotted lines).

The duration of the different stages changes when the pump fluence is varied, but otherwise the data are qualitatively quite similar. Examples illustrating the dependence on pump laser fluence are given in the next two figures, which show the measured SH (Fig. 2) and the *p*-polarized reflectivity of gallium arsenide (Fig. 3) above the melting threshold. As a consistent feature of the data we find that for all pump fluences the overall decay of the SH is always a factor of 2–3 faster than the rise of the reflectivity. This observation is in agreement with our previous^{8,30} and the results of others.^{6,7,9,14}

The measurements of the optical reflectivity in silicon reveal a very similar behavior of the temporal evolu-

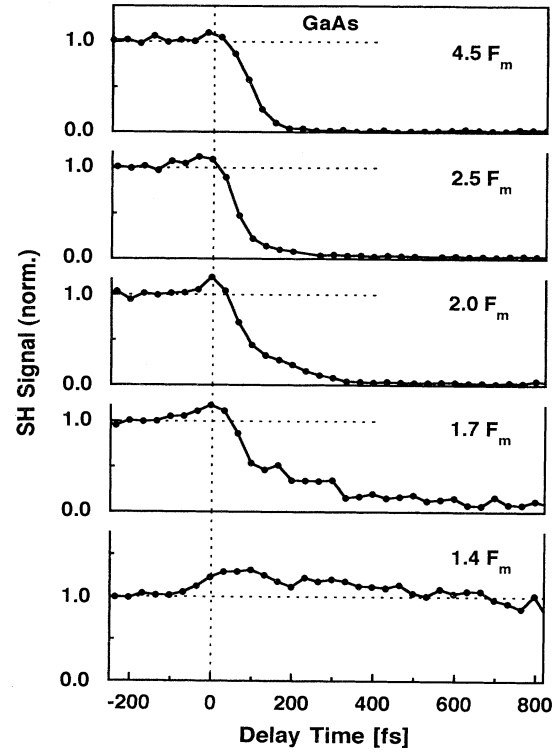


FIG. 2. *s*-polarized SH of gallium arsenide as a function of delay time for various fluences above the melting threshold. Pump fluences are normalized to the melting threshold $F_m = 0.17$ J/cm².

tion. Examples are shown in Fig. 4, which depicts the measured time dependence of the *p*-polarized reflectivity in silicon for different fluences above threshold. The melting threshold of silicon has been determined to be $F_m = 170$ mJ/cm², which is equal to the measured threshold value of gallium arsenide. Once again, two different stages of the evolution can be recognized, in complete analogy with the corresponding data of gallium arsenide (Figs. 1 and 3). For lower fluences the optical reflectivity does not approach a constant value during the first picosecond, because in this fluence regime the phase transition is due to the slow, thermal mechanism.^{8,31} On the other hand, for the highest fluences it takes only about 300 fs to reach the final stationary value of the optical reflectivity, which corresponds to the reflectivity of liquid silicon.

The *s*-polarized data for silicon are shown in Fig. 5. Again striking similarities of the behavior of silicon and gallium arsenide can be noticed. Compare, for example, the *s*-polarized reflectivity of gallium arsenide of Fig. 1 with the corresponding data of silicon ($1.8F_m$ and $2.2F_m$ in Fig. 5). Quite generally, it is evident from our data that the characteristics of the processes in silicon and gallium arsenide are very similar; e.g., the shape of the reflectivity curves is the same, the time constants for the different stages of the transformation are similar, and also the melting threshold is nearly the same.

Keeping in mind that close to the threshold the phase transformation is due to thermal melting and takes tens

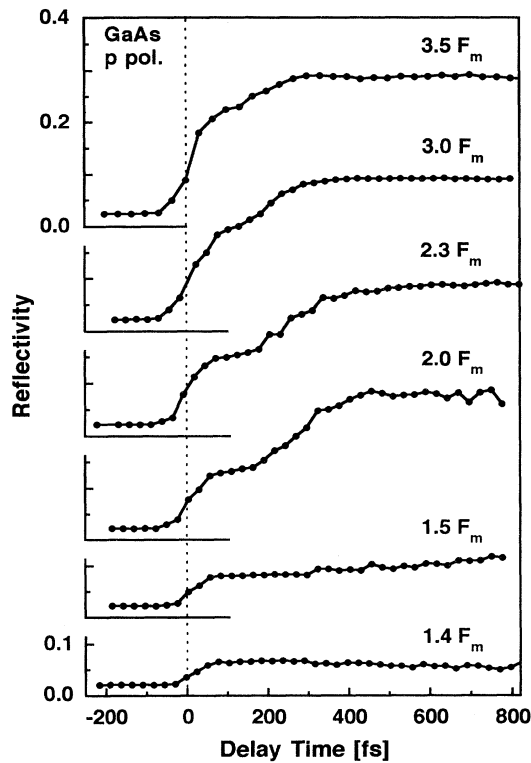


FIG. 3. p -polarized reflectivity of gallium arsenide as a function of delay time for various fluences above the melting threshold. Pump fluences are normalized to the melting threshold $F_m = 0.17 \text{ J/cm}^2$. Same experimental conditions as in Fig. 1.

of picoseconds to develop, no principal differences of the results for laser fluences slightly below and above F_m would be expected on a very short time scale, say during 1 ps after excitation. The data presented in Fig. 6 demonstrate that this is indeed observed. Shown is the p -polarized optical reflectivity of silicon for laser fluences ranging from $0.5F_m$ below threshold to $1.2F_m$ just above threshold (note the expanded vertical scale in Fig. 6). It can be seen that during the first picosecond after excitation the induced changes of the reflectivity slightly below and slightly above threshold are qualitatively very similar.

A fundamental shortcoming of experiments measuring the optical reflectivity at a single wavelength and a single angle of incidence is the difficulty to distinguish a dense electronic plasma of a highly excited solid from molten material such as liquid silicon and gallium arsenide having metallic properties. In order to overcome this ambiguity in identifying liquid and solid phases we have performed some reflectivity measurements as a function of the angle of incidence and wavelength.

Figure 7 shows an example of a measurement of the angular dependence of the optical reflectivity at 625 nm for silicon. The pump fluence and the probe pulse delay time were $F = 3F_m$ and 300 fs, respectively. The solid curves represent a least-squares fit of the data using the Fresnel formulas. The data can be fitted with optical constants $n = 3.1$ and $k = 5.2$, which are in agreement within

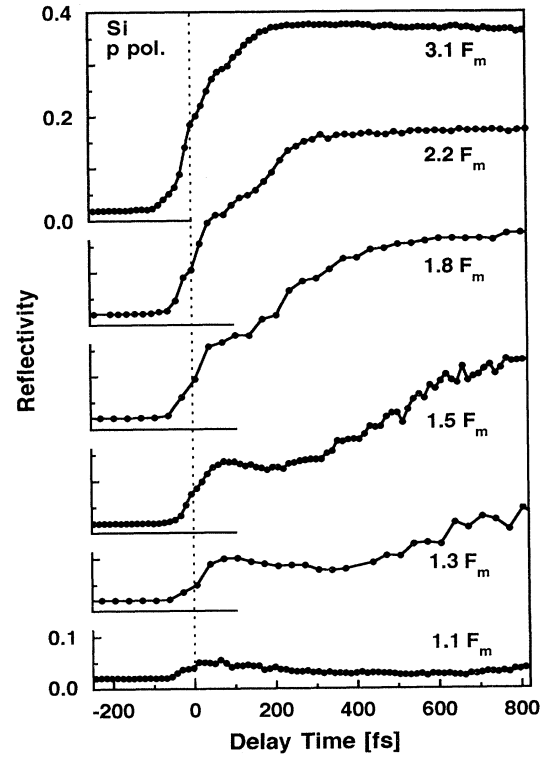


FIG. 4. p -polarized reflectivity of silicon as a function of delay time for various fluences above the melting threshold. Same conditions as in Fig. 1.

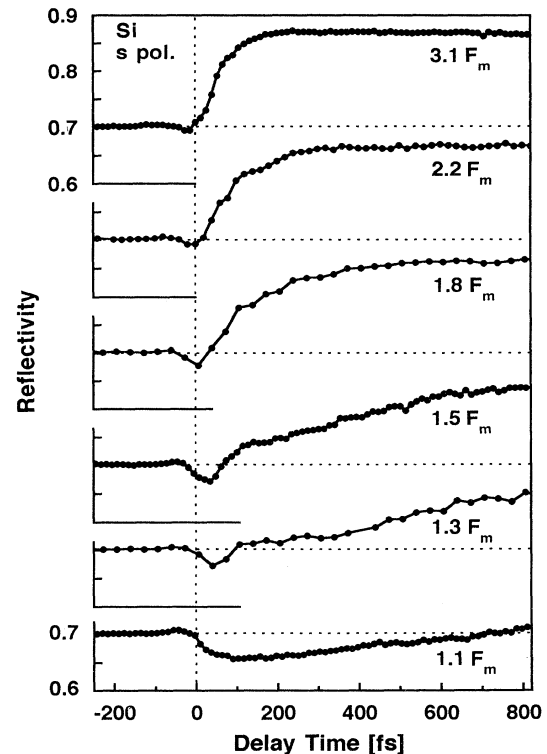


FIG. 5. s -polarized reflectivity of silicon as a function of delay time for various fluences above the melting threshold. Same conditions as in Fig. 1.

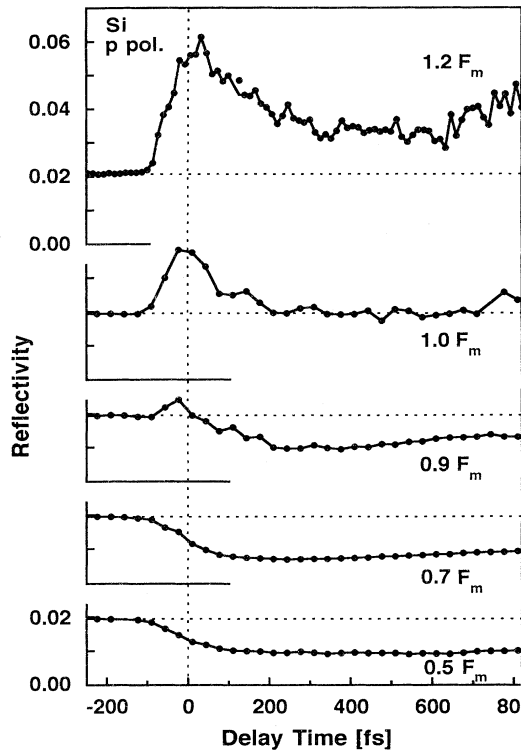


FIG. 6. p -polarized reflectivity of silicon as a function of delay time for various fluences below the melting threshold. Same conditions as in Fig. 1.

experimental accuracy with the known optical constants of liquid silicon.²⁸ The results for gallium arsenide were found to be very similar.

Finally, we present the measured time-resolved reflectivity spectra. The spectra for early times are expected to show features of the band structure of the solid,³² whereas for later times, after the transition to the final

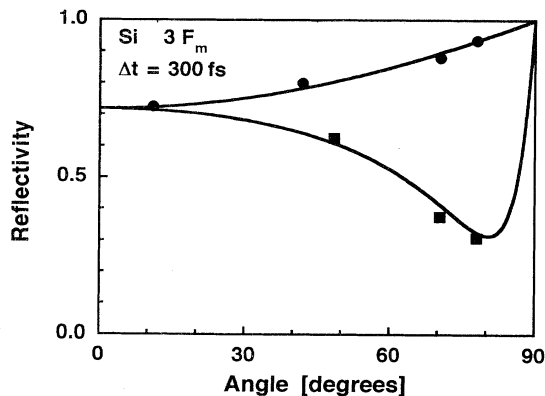


FIG. 7. Reflectivity of silicon as a function of the angle of incidence at 300 fs and an excitation fluence of $F = 3F_m$. Circles, s polarization; squares, p polarization; solid curves, least-squares fit of the Fresnel formula to the measured reflectivities. The extracted optical constants $n = 3.1$ and $k = 5.2$ are in agreement with the known optical constants of liquid silicon.

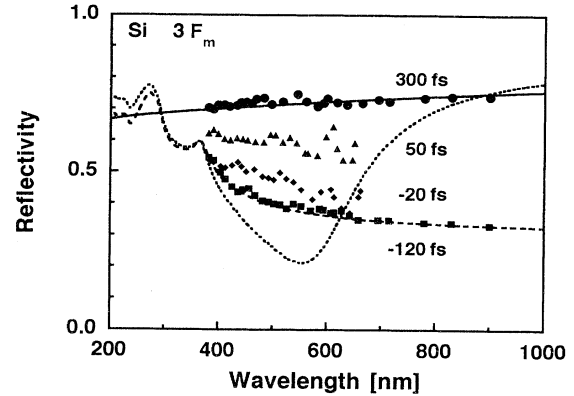


FIG. 8. Data points, measured spectra of the reflectivity of silicon for different delay times and s polarization; pump fluence, $F = 3F_m$; angle of incidence, 11° ; dashed curve, spectrum of the solid phase; solid curve, spectrum of the liquid phase.

liquid state, the spectra should be characteristic of the structure of a metal. Figure 8 shows examples of reflectivity spectra of silicon for four different delay times between the pump pulse and the white-light-continuum probe pulse. The pump fluence in this case was $3F_m$. The data indicate a continuous increase of the reflectivity over the entire range of wavelengths monitored in this experiment. Within experimental accuracy a decrease of the reflectivity that might be expected to result from the photoexcited electron-hole plasma was not observed. This observation is in agreement with the single-wavelength measurements presented earlier. The initial dip in the s -polarized reflectivity observed around zero delay at lower fluences (compare Fig. 5) disappears at the high fluences. The data and the various curves in Fig. 8 will be discussed in more detail in Sec. V.

IV. ANALYSIS OF THE DATA

The data presented in the preceding section reveal a quite complicated picture of the temporal evolution of optical reflectivity and SH, suggesting that the observed signals are affected by a variety of different processes. In order to extract information on the laser-induced phase transformation we undertook a careful analysis of the data to derive the *optical constants* (complex index of refraction) and the *nonlinear optical susceptibility*. These quantities represent the basic changes of the material properties underlying the observed evolution of reflectivity and the SH. Because of the rather complicated functional dependences between the observable quantities and the basic material properties, a careful analysis of the data in terms of the basic material properties turns out to be very important.^{33,34}

First, let us discuss the treatment of the reflectivity data. Having measured the optical reflectivity both for s and p polarization, the optical constants of the material can be calculated by numerically inverting the Fresnel formula. Starting with the known complex refrac-

tive index^{35,36} of the unperturbed material, we adopt a simple trial and error algorithm to obtain a pair of n and k , which gives the best approximation of the measured reflectivities. An example is shown in Fig. 9 for gallium arsenide well above threshold ($F = 3.5F_m$) and in Fig. 10 for silicon slightly below threshold (data of Fig. 6: $F = 0.9F_m$).

A general common feature of the data is a strong decrease of the refractive index n and a strong increase of the extinction coefficient k during the first 100 fs. Above threshold both n and k finally approach the optical constants of the liquid phase, marked by the dash-dotted lines in Fig. 9. Below threshold the initial changes of n and k relax with a time constant of ≈ 1 ps (silicon). In Fig. 10 the different positions of the minimum of n ($\Delta t \approx 100$ fs) and the maximum of k ($\Delta t \approx 0$ fs) should be noted. Being observed only in silicon near threshold, this feature is probably related to the dominance of nonlinear absorption in this material.

It should be pointed out that near the principal angle of incidence the response to changes of the optical constants differs greatly for the two polarizations. For s polarization a decrease (increase) of either n or k leads to a decrease (increase) of the reflectivity. Thus, despite strong changes of n and k during the first 100 fs, only a relatively small drop in the s -polarized reflectivity is produced at early times because the changes partially cancel each other. For the longer times and higher fluences the increase of k dominates, the net effect being a rise of the reflectivity.

The response of the p -polarized reflectivity to changes in n and k is more complicated. The changes of the reflectivity are strongly dependent on the difference between the angle of incidence and the actual principal angle of incidence, which varies with the optical constants. For low values of k the principal angle of incidence is mainly determined by the refractive index n .

A change of k alone always results in a change of the reflectivity in the same direction, like in the case of s polarization. However, a change of n results in a change of the reflectivity in the same direction only when the

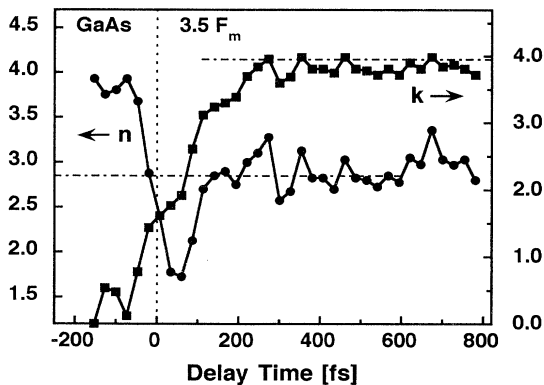


FIG. 9. Optical constants of gallium arsenide as a function of time, derived from the reflectivity data for $F = 3.5F_m$. Dash-dotted lines, optical constants of liquid gallium arsenide. For unperturbed crystalline gallium arsenide $n = 3.87$, and $k = 0.2$.

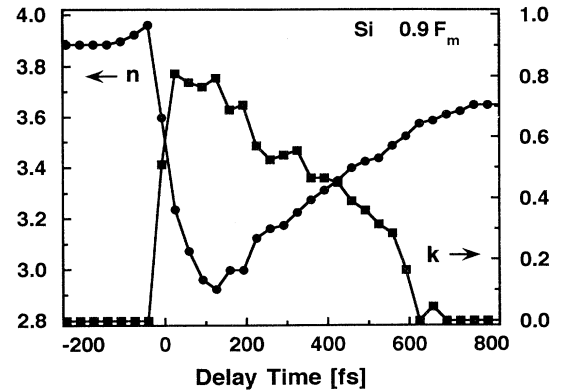


FIG. 10. Optical constants of silicon as a function of time, derived from the reflectivity data for $F = 0.9F_m$. For unperturbed crystalline silicon $n = 3.885$, and $k = 0.017$.

principal angle is the larger of the two angles. The situation can be quite complicated for other values of the angles. For example, when the two angles are equal, the p -polarized reflectivity $R_{||}$ is insensitive to changes of n because $dR_{||}/dn = 0$ at the principal angle.

To illustrate the behavior near the principal angle of incidence consider the data of Figs. 1 and 9 for gallium arsenide. The principal angle of incidence of the unexcited material is 76° , greater than the angle of incidence 70.5° . The excitation by the pump pulse leads to a drop of the refractive index; e.g., near zero delay time the index has dropped to a figure of about 2.5. This value corresponds to a principal angle of 71° , which is now close to the actual angle of incidence. The expected decrease of the reflectivity due to this change of the principal angle is masked by the simultaneous increase of k . While for the s polarization the decrease of n dominates over the rise of k , this is not the case for p polarization because of the weak response of the reflectivity to changes of n near the principal angle of incidence. The result of these competing effects is the observed decrease for s polarization and the simultaneous increase for p polarization.

Similar arguments explain the differences of the time dependences of the p -polarized reflectivity in silicon below the melting threshold (Fig. 6). According to Fig. 10 the pump pulse produces a sharp decrease of n and an increase of k . For the two lowest fluences in Fig. 6 the reflectivity is dominated by the changes of n and the resulting change of the principal angle, lowering the reflectivity. While too small to play a role for the very low fluences, k becomes dominant for stronger excitation, causing an initial increase of the reflectivity at higher fluences. For later times, however, k reaches a maximum, while n is further decreasing, running through a minimum after the maximum of k . The result is a decrease of the reflectivity after the initial rise.

After this somewhat laborious discussion of the reflectivities and optical constants, we wish to examine the influence of the latter on second-harmonic generation and analyze our SH data for gallium arsenide. Using well known formulas of nonlinear optics,³⁷ the SH signal generated by the probe pulse can be written as

$$S_{\perp,2\omega} \propto \int_{-\infty}^{\infty} \left| \chi_{eff}^{(2)} \right|^2 \left| \frac{t_{\parallel,\omega}^2 \sin \theta_{\omega} \cos \theta_{\omega}}{(n_{2\omega} \cos \theta_{2\omega} + \cos \theta)(n_{2\omega} \cos \theta_{2\omega} + n_{\omega} \cos \theta_{\omega})} \right|^2 |E_{0,\omega}^2|^2 dt. \quad (1)$$

Here $S_{\perp,2\omega}$ is the s -polarized SH signal, $E_{0,\omega}^2$ represents the p -polarized electric field of the probe pulse, and $\chi_{eff}^{(2)} = \chi_{xyz}^{(2)}$ is the effective tensor element of the second-order nonlinear susceptibility; otherwise the following notation is used: $t_{\parallel,\omega}$ is the Fresnel transmission coefficient, θ is the angle of incidence, θ_x is the angle of refraction, and n_x is the complex index of refraction where $x = \omega$ or 2ω .

The SH is expected to vanish during the phase transformation from the crystalline to the liquid state because the latter is centrosymmetric and $\chi^{(2)}$ is zero by symmetry. However, the time dependence of the SH due to the changes and the final vanishing of $\chi^{(2)}$ is obscured by changes of the second factor of the integrand in (1). This term depends *only on the linear optical properties* of the material, both explicitly and implicitly via the refraction angles θ_{ω} and $\theta_{2\omega}$. Thus it is clear that changes of the optical constants caused by the pumping process will lead to changes of the SH, even if $\chi^{(2)}$ does not vary at all.

The strong effect of the variation of the optical constants on the SH is illustrated in Fig. 11. The dashed curve shows same SH data as Fig. 1. These raw data are compared with the calculated SH signal, which takes into account the experimentally determined variation of the complex index of refraction and assumes that $\chi^{(2)}$ is *constant*. Possible changes of the optical constants at 2ω have been neglected.

The result is shown by the dotted curve in Fig. 11. The comparison of the dashed and dotted curve indicates surprisingly large changes of the SH signal solely caused by the laser-induced variations of the linear optical properties. In particular, it turns out that the very large peak of the calculated SH is due to the initial decrease of the refractive index n discussed above.

With the knowledge of the optical constants we can now correct the SH raw data and obtain the underlying change of $\chi^{(2)}$. The resulting $\chi^{(2)}$ is given by the solid line. The correction procedure reveals a very strong and extremely fast initial drop of $\chi^{(2)}$ within the first 100fs, followed by a more gradual decrease over a few hundred femtoseconds.

The data obtained for other values of the laser fluence have been analyzed in a similar way. The inset of Fig. 11 shows an example of the time dependence of $\chi^{(2)}$ for a lower fluence $1.5F_m$. This is the fluence regime of slow, ordinary thermal melting,⁸ in which the structural changes develop on a time scale of tens of picoseconds. Nevertheless, we observe a very sharp drop of $\chi^{(2)}$ within the first 100fs and a constant level during the remaining time.

It should be emphasized that such an initial rapid decrease of $\chi^{(2)}$ is a characteristic feature of all our data, both above and below threshold. However, there are important differences of the *subsequent* time dependence of

$\chi^{(2)}$ for the different fluence regimes. For fluences below and up to about 20–30 % above threshold a *recovery* of $\chi^{(2)}$ to the value of the unperturbed solid is observed on a time scale of 2–3 ps. Of course, SH generation ultimately disappears above threshold, but on a very much longer time scale of several tens of picoseconds, which is given by the time for the formation of a liquid overlayer by thermal melting. On the other hand, in the high fluence regime $\chi^{(2)}$ *does not recover*. Instead, the nonlinear susceptibility disappears completely within a few hundred femtoseconds. The characteristic time of this final decay shortens with increasing fluence.

Our observations of the high fluence regime are, in principle in agreement with the results reported in Ref. 9, where an ultrafast quenching of $\chi^{(2)}$ within the probe pulse duration was found for $4F_m$. However, at such a high fluence it was not possible to distinguish the initial rapid drop and the final decay of $\chi^{(2)}$, probably because the processes are too fast to be time resolvable.

Before turning to the discussion of the results, an underlying approximation of our procedure to calculate the optical constants from the reflectivity should be mentioned. Our analysis treats the material as spatially homogeneous, neglecting the spatial variation of the optical properties in the depth of the excited material. In principle the depth profile of the optical properties should be taken into account.³⁸ However, the excitation profile and the variation of the optical properties are not well

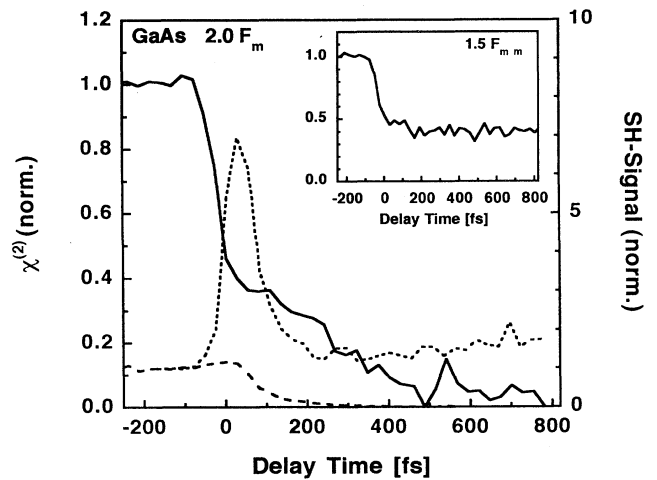


FIG. 11. Measured reflected second harmonic of the probe pulse (dashed curve, same as in Fig. 1), the calculated SH (dotted curve, see the text) and the measured nonlinear susceptibility $\chi^{(2)}$ of gallium arsenide as a function of time for $F = 2F_m$. The inset shows the measured time dependence of $\chi^{(2)}$ for a lower pump fluence, $F = 1.5F_m$.

known and a more accurate analysis including the effect of spatial inhomogeneity is very difficult. It follows that the experimentally determined optical constants must be interpreted as spatial averages over the absorption depth. Fortunately, k is strongly increasing upon excitation and the effect of spatial averaging is reduced because the probe pulse penetrates only a small fraction of the excited depth. As far as the SH is concerned, spatial averaging is expected to be of minor importance because in this case the probe depth is given by the absorption depth at 2ω , which is much less than the thickness of the excited material layer. The effect of spatial averaging in the determination of the linear optical constants leads to some underestimate of the changes of $\chi^{(2)}$.

V. DISCUSSION

It has been pointed out several times that the observed characteristics of the phase transformation in silicon and gallium arsenide are very similar. In particular, according to our measurements and those of others,^{5,7} the melting thresholds are very nearly the same. This appears to be surprising at first glance because the linear absorption at 625 nm of silicon ($\alpha = 3.5 \times 10^3 \text{ cm}^{-1}$) and gallium arsenide ($\alpha = 4.3 \times 10^4 \text{ cm}^{-1}$) differ by approximately one order of magnitude. A plausible explanation is that *non-linear* absorption processes must be taken into account to explain the observed thresholds. Kütt *et al.*³⁹ and Reitze *et al.*⁴⁰ have derived a two-photon absorption coefficient of $\beta \approx 40 \text{ cm/GW}$ at $\hbar\omega = 2 \text{ eV}$ from reflectivity measurements on silicon below the melting threshold. From our own measurements we have obtained a somewhat higher value of $\beta \approx 55 \text{ cm/GW}$.⁴¹ Thus the effective absorption coefficient of silicon at the measured melting threshold (170 mJ/cm^2) is $\alpha_{\text{eff}} = \alpha_{\text{lin}} + \beta(1 - R)I_{\text{max}} \approx (3-5) \times 10^4 \text{ cm}^{-1}$. This value is comparable with the linear absorption of gallium arsenide, indicating that at intensities corresponding to the threshold the effective optical absorption in both materials is comparable.

Other physical differences of the two materials, e.g., differences of the electronic structure and of the relaxation mechanisms of the photoexcited carriers, apparently do not substantially affect the process of ultrafast disordering. It is therefore possible to drop explicit reference to silicon or gallium arsenide in most of the following discussion.

A. Two-step model

A crude comparison of the data reveals that the second harmonic generally changes faster than the optical reflectivity. For example, it can be seen from Fig. 1 that the SH disappears in about 200 fs, whereas the reflectivity takes roughly 500 fs to rise to the final value. Some authors^{9,14,20} have proposed an intermediate nonmetallic phase with centrosymmetric (gallium arsenide^{9,20}) or isotropic (silicon¹⁴) structural symmetry to explain that the SH disappears before the reflectivity reaches the value corresponding to the disordered liquid state.

On the other hand, the more detailed examination of the data of Secs. III and IV has provided clear evidence of two distinct regimes in the evolution of the SH and the optical reflectivity. For both the SH and the reflectivity there is a first stage of very short duration, comparable with the duration of the laser pulses, followed by a second stage in which the changes of the reflectivity and the SH are relatively slow. Still better than in the raw data the two different stages of the evolution manifest themselves in the actual change of the nonlinear susceptibility as shown in Fig. 11. An important point to recall here is that the initial drop of the nonlinear susceptibility is observed for laser fluences both above and below the melting threshold (compare solid curve and insert in Fig. 11). Furthermore, only the *amount* of change in the first stage is dependent on the laser fluence, but not its *duration*, which is always given by the duration of the pump pulse. These observations can be readily understood if electronic excitation by the laser pump pulse is causing the effect. On the other hand, if some structural rearrangement were invoked to explain the initial fast changes of the SH, the duration of this process⁴² would not necessarily be limited by the laser pulse width. Thus the most likely explanation of the initial rapid changes of the SH is, in our opinion, the strong electronic excitation during the interaction with the pump pulse.

This leads us to propose a simple phenomenological two-step model of the laser-induced order-disorder transition. There is the initial *excitation stage* in which the changes of the SH and the optical reflectivity are caused by electronic excitation of the structurally intact solid material, followed by the proper *transition stage* in which the material undergoes a structural change towards the disordered liquid phase. The excitation stage is limited by the duration of the laser pulse, whereas the transition stage develops on a longer time scale of several hundred femtoseconds or even longer, depending on the actual strength of the laser excitation.

The two-step model also provides a consistent interpretation of the observed changes of the optical reflectivity, both above and below threshold. The reflectivity data just below threshold are representative of the reflectivity changes directly caused by electronic excitation during the excitation stage (see, e.g., Fig. 6). The optical reflectivity above threshold on the other hand, is composed of some contribution of short duration resulting from electronic excitation, very similar to the corresponding data below threshold and an additional component due to the phase transformation, which rises monotonously to the reflectivity of the liquid.

B. Excitation stage

The properties and the dynamics of optically excited carriers in semiconductors have been studied extensively during the past two decades.⁴³ However, the extremely high densities and temperatures such as those encountered during the excitation stage prior to the phase transformation have rarely been investigated so far. Most previous studies, for example, were limited to the density

regime below 10^{20} cm^{-3} . Nevertheless, some basic guidelines and conclusions concerning the changes of the optical properties associated with hot, dense electron-hole plasmas can be deduced from the previous low density work.

The density of excited electron-hole pairs created during the excitation stage can be roughly estimated from the density of absorbed optical energy, i.e., $N_{e-h} \approx (1 - R)\alpha_{\text{eff}}F/\hbar\omega_0$. From the experimental parameters $\hbar\omega_0 = 2 \text{ eV}$, $R = 35\%$, and $\alpha_{\text{eff}} \approx (3-5) \times 10^4 \text{ cm}^{-1}$ we obtain $N_{e-h} \approx (0.5-1) \times 10^{22} \text{ cm}^{-3}$ at the melting threshold. Of course, for higher fluences $F > F_m$ still higher electron-hole densities are achieved. This estimate suggests that the density of photoexcited electron-hole pairs can readily exceed a figure corresponding to 10% of the total number of valence electrons $N_{\text{total}} \approx 2 \times 10^{23} \text{ cm}^{-3}$.

The effective excess energy of the electron-hole pairs is greater than the single-photon excess energy $\hbar\omega_0 - E_{\text{gap}}$ because of the strong two-photon and/or free-carrier contributions to the optical absorption. The initial electronic energy distribution relaxes to a thermal distribution within a few tens of femtoseconds^{44,45} due to ultrafast carrier-carrier scattering. Thus the initial carrier temperature should be roughly of the order of 10^4 K .

1. Changes of the linear optical properties

The principal physical effects responsible for the changes of the linear optical response caused by very strong electronic excitation are the following: (i) state and band filling,^{46,47} (ii) renormalization of the band structure,⁴⁸ and (iii) free-carrier effects. Due to the very high electronic temperature the photoexcited carriers are distributed over a wide range of the Brillouin zone, which tends to reduce the changes of the population experienced by the optically coupled states at any particular probe wavelength. Under these circumstances it is possible to approximate the effect of band renormalization as a rigid shift of the band structure,⁴⁹ leading to a reduction of the band gap. The changes of the optical properties caused by this reduction can be roughly estimated from a corresponding spectral shift of the optical spectra. The band gap shrinkage for silicon⁵⁰ extrapolated to $N_{e-h} = 10^{22} \text{ cm}^{-3}$ is $\Delta E = 400 \text{ meV}$, suggesting changes of the optical constants³⁶ of $\Delta k = +0.02$ and $\Delta n = +0.3$.

The changes of the optical properties caused by the optical response of the free carriers can be described by the Drude model.⁵¹ Only rough estimates can be obtained because the basic Drude parameters, the optical reduced mass m_{opt}^* and the damping time τ_D , depend on temperature and density and are not accurately known for our experimental conditions. Nevertheless, the Drude model predicts, qualitatively speaking, a decrease of the refractive index n and an increase of the extinction coefficient k at a probe wavelength of 625 nm.

The strong decrease of n and the strong increase of k observed experimentally both for silicon and gallium arsenide suggest that the optical response of the excited semiconductors is dominated by free-carrier effects. Only

at the very beginning of the excitation process a slight increase of n has been observed (see Fig. 10), which could be due to shrinkage of the band gap. The sharp increase of k around zero delay time (Fig. 10) can be attributed to pump-induced two-photon absorption.

2. e-h relaxation

Assuming that the contributions from band and state filling are relatively small, they will be neglected in the following and the Drude model will be used to calculate the time dependence of carrier density and relaxation time from the measured optical constants. Because of the uncertainties of the optical reduced mass, only the ratio N_{e-h}/m_{opt}^* can be extracted from the data. A result for silicon slightly below threshold ($F = 0.9 \times F_m$) is depicted in Fig. 12, where N_{e-h}/m_{opt}^* and $1/\tau_D$, derived from the data of Fig. 10, are plotted as a function of delay time (solid and dotted line, respectively). The dashed line in Fig. 12 shows the evolution of N_{e-h}/m_{opt}^* when the estimated contributions to the changes of the optical constants due to gap shrinkage and lattice heating are taken into account.

With an optical mass between 0.15 and 0.5 of the free-electron mass,^{52,53} a maximum initial electron-hole density between $5 \times 10^{21} \text{ cm}^{-3}$ and $1.5 \times 10^{22} \text{ cm}^{-3}$ is estimated. These figures are in good agreement with the rough estimate of N_{e-h} based on the optically absorbed laser energy.

The data indicate that the initial electron-hole density relaxes in about 1 ps. We believe that this figure is accurate within a factor of 2, due to the various assumptions and approximations. Despite these uncertainties it appears that the observed relaxation of the carrier concentration is too fast to be explained by Auger recombination alone. The Auger recombination coefficient is expected to decrease as a result of screening and the Auger recombination time should approach a constant value of approximately 6 ps at densities

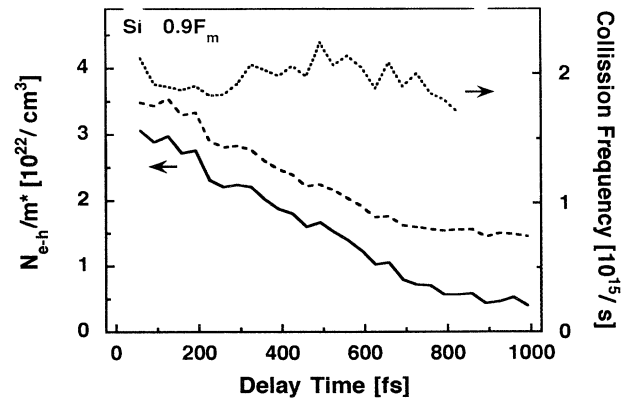


FIG. 12. Time dependence of the density (N_{e-h}/m_{opt}^* , solid line) and the Drude damping constant ($1/\tau_D$, dotted line) of an $e-h$ plasma in silicon derived from the optical constants of Fig. 10. The dashed line is the density including an estimated correction for gap shrinkage and lattice heating.

above 10^{21} cm^{-3} .⁵⁴ Other possibilities include plasmon-phonon-assisted recombination⁵⁵ as a very fast relaxation channel at high densities and diffusion of the carriers into the bulk.^{5,56–58} Nonlinear absorption leads to a significant enhancement of the diffusion in silicon at high excitation because nonlinear absorption produces much steeper carrier density profiles than linear absorption. Modeling the density profile including nonlinear absorption, a time constant of 1–2 ps is estimated for the relaxation of the carrier concentration due to diffusion, which is in good agreement with the experimental data. Thus we believe that the observed fast-carrier relaxation is probably caused by diffusion.

The values of $1/\tau_D$ up to $\approx 2 \times 10^{15} \text{ s}^{-1}$, derived from our data, are in agreement with the results of other groups.^{59,60} These rates are very fast compared with the carrier-phonon collision rates ($10^{12} - 10^{13} \text{ s}^{-1}$), which dominate the current relaxation at low densities. Theoretical work^{61,62} has explained these fast damping rates as being due to electron-hole collisions in which the total momentum is conserved, but not the current.

3. Changes of the nonlinear optical properties

In the framework of the bond charge model^{63,64} the principal contribution to the nonlinear optical response of polar semiconductors has been attributed to the asymmetry of the bond charge between adjacent atoms (in our case gallium and arsenic). The application of the bond charge model is, strictly speaking, limited to optical frequencies below the fundamental gap ($2\omega_0 < E_{\text{gap}}/\hbar$). A decrease of $\chi^{(2)}$ may nevertheless be expected to result from a depletion of the bond charge during strong optical interband excitation. Changes of $\chi^{(2)}$ could also arise from band-gap shrinkage at high electron-hole concentration. The effect of band-gap shrinkage can be estimated from the frequency dependence of the nonlinear susceptibility. Experimental^{65–67} as well as theoretical^{68,69} work indicate strong dispersion of $\chi^{(2)}$ in gallium arsenide in the frequency range of interest. The experimental data⁶⁷ reveal a maximum of $\chi^{(2)}$ near 2 eV, which corresponds to the photon energy of the probe pulses in our experiments and a decrease down to approximately 50% of the maximum at 2.5 eV. Thus both bond-charge depletion and band-gap shrinkage, which are expected to lead to a decrease of $\chi^{(2)}$ upon strong electronic excitation, could explain the experimentally observed fast decrease of $\chi^{(2)}$ during the excitation phase. For both mechanisms the magnitudes, but not the time constants, would be expected to vary with laser fluence, in agreement with the observed fluence dependence of the initial decay of $\chi^{(2)}$. In our opinion these purely electronic mechanisms are more likely than structural changes of the material to explain the observed fast changes of $\chi^{(2)}$ during the excitation stage.

C. Transition stage

The excitation stage is followed by a transformation of the excited solid to a disordered liquidlike state provided

the threshold fluence for melting is exceeded. Within a fluence range up to about 1.3 times the threshold value the structural transformation develops on a time scale of several tens of picoseconds. As pointed out above, this relatively slow transformation near threshold is due to thermal melting^{8,31} under highly superheated conditions.⁷⁰

On the other hand, it appears that some fundamentally different type of transformation occurs for fluences exceeding 2–3 times the threshold. In this high fluence regime the optical reflectivity measured at a single probe wavelength reaches a value corresponding to the liquid state in less than 1 ps. Our more detailed reflectivity measurements in which the angle of incidence and the wavelength were varied have confirmed that in both materials the optical properties approach the values corresponding to the liquid state in less than 1 ps after excitation. For example, the angular reflectivity spectrum of silicon at 300 fs (Fig. 7) measured for a pump fluence of $F = 3F_m$ can be fitted using the known optical constants of liquid silicon at 625 nm. The frequency spectra of the reflectivity of silicon measured for the same fluence (Fig. 8) show that the change from the solid spectrum (dashed line) to the spectrum of the liquid (solid line) is complete at 300 fs. In addition, the properly corrected SH data for gallium arsenide indicate that in the high fluence regime $\chi^{(2)}$ disappears, dropping from its reduced value at the end of the excitation stage below the detection limit in a few hundred femtoseconds. The final maximum reflectivity is independent of the laser fluence and constant for a few nanoseconds until resolidification occurs. These observations are in agreement with the behavior that would be expected if the phase established at the end of the transition stage was the liquid phase.

These various experimental results support the conclusion that at sufficiently high excitation the materials undergo—after some distinct excitation stage—a direct structural transformation to the liquid state within a few hundred femtoseconds, without passing through intermediate nonmetallic phases with different structural properties. As discussed previously, the time of this transition is shorter than the relaxation time, ruling out thermal mechanisms as an explanation of the structural transformation.

There is a long history^{16–22} of the possible role of a nonthermal mechanism in laser-induced structural transformations of covalent semiconductors. The extremely high concentration of photoexcited free carriers plays a crucial role in these concepts. It is well known that free carriers may cause some softening of TA-phonon modes²³ to the extent that the cold lattice becomes unstable against shear stress at some critical carrier density around a few times 10^{22} cm^{-3} . Plasma-induced transitions are very unlikely to play a role for laser pulses much longer than the relaxation times of the material. However, the model of plasma-induced melting has been proposed as an explanation of phase transformations induced by ultrashort *femtosecond* laser pulses.^{7,9,14,20,21}

Recently, Stampfli and Bennemann²¹ have developed a dynamical theory in which a tight-binding formalism was used to investigate the stability of the lattice as a func-

tion of plasma density in silicon. They have studied the change of the mean atomic displacement as a function of time under the influence of the carrier plasma. It has been shown that the mean displacement may increase to approximately 1 Å within 100–200 fs, nearly half the equilibrium bond length (2.35 Å), which is clearly sufficient to destroy the lattice. An interesting aspect of this model is that it predicts an effective repulsive potential in which the lattice atoms gain kinetic energy more rapidly than in ordinary electron-phonon collisions. As a result, disordering and heating of the material could occur much faster than in a normal thermalization process due to electron-phonon interaction.

At the present time a direct, detailed comparison of this new model with the experimental data is not possible because the changes of the linear and nonlinear optical properties accompanying the transition have not been calculated as yet. Siegal *et al.*³⁴ have recently used a simple oscillator model to describe the observed changes of the optical properties during femtosecond laser-induced phase transformation in gallium arsenide. Their measurements could be interpreted in terms of a single oscillator dielectric function having a resonant frequency that decreases as a function of pump fluence. The resonance frequency was interpreted as the average optical gap of the material. According to this picture the transition to a metallic state occurs when the average optical gap is reduced to the point where the conduction-band minimum drops below the valence-band maximum.

The discussion is concluded by a qualitative comparison of plasma-assisted and ordinary thermal melting. In a thermal melting process the atoms must gain kinetic energy by successive electron-phonon collisions to overcome the binding potential of the stable crystalline structure. The collisional exchange of energy between electrons and atoms requires a relatively long time of several picoseconds. On the other hand, the generation of an *e-h* plasma exceeding some characteristic critical density instantaneously turns the initial binding potential into a repulsive potential, permitting lattice atoms to change coordination and gain kinetic energy in a time of the order of a vibrational period, which is of the order of 100 fs. The plasma-assisted process bears some analogy with the photodissociation of molecules. For intermediate fluences both the thermal process and the plasma-assisted

process are likely to contribute to bring about the structural change.

VI. SUMMARY AND CONCLUSIONS

Laser-induced phase transitions in silicon and gallium arsenide have been studied by means of femtosecond time-resolved measurements of the optical reflectivity and of the reflected second harmonic. These experiments have provided the changes of the linear optical constants and of the second-order nonlinear optical susceptibility. It has been shown that the reflected SH is very strongly affected by the changes of the linear optical constants and that these effects must be taken into account to derive the nonlinear susceptibility from SH data.

The observed evolution of the linear and nonlinear optical properties suggest a two-step model of the laser-induced phase transformation: During and shortly after the laser excitation pulse the optical constants and the nonlinear susceptibility of the material are determined by the strong electronic excitation, in particular, the generation and relaxation of a photoexcited dense electron-hole plasma. We have called this stage the *excitation stage*. The actual transformation of the crystalline solid to a metallic liquid occurs during the subsequent *transition stage*. The duration of the latter has been observed to be dependent on the strength of the laser excitation. For fluences of approximately three times the threshold fluence the duration of the transition stage is 300 fs. Our data provide further evidence that for excitation fluences leading to electron-hole densities in excess of 10^{22} cm⁻³, a nonthermal electronic mechanism gives rise to an ultrafast (subpicosecond) transformation from the covalent crystalline to the metallic liquid state.

ACKNOWLEDGMENTS

We are grateful to P. Stampfli and K.H. Bennemann for making their results available to us prior to publication and to Wacker Chemitronic, Burghausen (Germany), for supplying the semiconductor wafers. Support of this work by the Deutsche Forschungsgemeinschaft within the program "Dynamik Optischer Anregungen in Festkörpern" is gratefully acknowledged.

¹ I.B. Khaibullin, E.I. Shtyrkov, M.M. Zaripov, R.M. Bayazitov, and M.F. Galjantdinov, *Radiat. Eff.* **36**, 225 (1979).

² For a review see R.F. Wood, C.W. White, and R.T. Young, *Pulsed Laser Processing of Semiconductors, Semiconductors and Semimetals* Vol. 23 (Academic, Orlando, 1984).

³ For a review see S.A. Akhmanov, N.I. Koroteev, and I.L. Shumay, *Nonlinear Optical Diagnostics of Laser-Excited Semiconductor Surfaces, Laser Science and Technology* Vol. 2 (Harwood Academic, London, 1989).

⁴ See, for example, D. von der Linde, in *Resonances — A Volume in Honor of the 70th Birthday of Nicolaas Bloembergen*, edited by M.D. Levenson, E. Mazur, P.S. Pershan,

and Y.R. Shen (World Scientific, Singapore, 1990), and references therein.

⁵ C.V. Shank, R. Yen, and C. Hirlimann, *Phys. Rev. Lett.* **50**, 454 (1983).

⁶ S.V. Govorkov, I.L. Shumay, W. Rudolph, and T. Schröder, *Opt. Lett.* **16**, 1013 (1991).

⁷ P. Saeta, J.-K. Wang, Y. Siegal, N. Bloembergen, and E. Mazur, *Phys. Rev. Lett.* **67**, 1023 (1991).

⁸ K. Sokolowski-Tinten, H. Schulz, J. Bialkowski, and D. von der Linde, *Appl. Phys. A* **53**, 227 (1991).

⁹ S.V. Govorkov, T. Schröder, I.L. Shumay, and P. Heist, *Phys. Rev. B* **46**, 6864 (1992).

- ¹⁰ D.H. Reitze, H. Ahn, X. Wang, and M.C. Downer, *Phys. Rev. B* **40**, 11986 (1990).
- ¹¹ D.H. Reitze, H. Ahn, and M.C. Downer, *Phys. Rev. B* **45**, 2677 (1992).
- ¹² D.H. Reitze, H. Ahn, X. Wang, and M.C. Downer, in *Ultrafast Phenomena VII*, edited by C.B. Harris, E.P. Ippen, G.A. Mourou, and A. Zewail, Springer Series in Chemical Physics Vol. 53 (Springer, Berlin, 1990).
- ¹³ C.V. Shank, R. Yen, and C. Hirlimann, *Phys. Rev. Lett.* **51**, 900 (1983).
- ¹⁴ H.W.K. Tom, G.D. Aumiller, and C.H. Brito-Cruz, *Phys. Rev. Lett.* **60**, 1438 (1988).
- ¹⁵ H.W.K. Tom, T. F. Heinz, and Y. R. Shen, *Phys. Rev. Lett.* **51**, 1983 (1983).
- ¹⁶ J.A. Van Vechten, R. Tsu, and F.W. Saris, *Phys. Lett.* **74A**, 422 (1979).
- ¹⁷ M. Wautelet and L.D. Laude, *Appl. Phys. Lett.* **36**, 197 (1980).
- ¹⁸ J. Bok, *Phys. Lett.* **84A**, 448 (1981); M. Combescot and J. Bok, *Phys. Rev. Lett.* **48**, 1413 (1982).
- ¹⁹ Yu.V. Kopaev, V.V. Menyailenko, and S.N. Molotkov, *Fiz. Tverd. Tela (Leningrad)* **27**, 3288 (1985) [*Sov. Phys. Solid State* **27**, 1979 (1985)].
- ²⁰ S.V. Govorkov, V.I. Emel'yanov, and I.L. Shumay, *Laser Phys.* **2**, 77 (1992).
- ²¹ P. Stampfli and K.H. Bennemann, *Phys. Rev. B* **42**, 7163 (1990); *Prog. Surf. Sci.* **35**, 161 (1991); *Phys. Rev. B* **46**, 10 686 (1992); **49**, 7299 (1994).
- ²² S. Das Sarma and J.R. Senna, *Phys. Rev. B* **49**, 2443 (1994).
- ²³ V. Heine and J.A. Van Vechten, *Phys. Rev. B* **13**, 1622 (1976).
- ²⁴ R. Biswas and V. Ambegaokar, *Phys. Rev. B* **26**, 1980 (1982).
- ²⁵ H. Schulz and D. von der Linde, *SPIE Proc.* **1268**, 30 (1990).
- ²⁶ P.M. Fauchet, *IEEE J. Quantum Electron* **25**, 1072 (1989).
- ²⁷ B. Danielzik, P. Harten, K. Sokolowski-Tinten, and D. von der Linde, in *Fundamentals of Beam-Solid Interactions and Transient Thermal Processing*, edited by M. J. Aziz, L. E. Rehn, and B. Stritzker, MRS Symposia Proceedings No. 100 (Materials Research Society, Pittsburgh, 1988), p. 471.
- ²⁸ K.M. Shvarev, B.A. Baum, and P.V. Gel'd, *Fiz. Tverd. Tela (Leningrad)* **16**, 3246 (1974) [*Sov. Phys. Solid State* **16**, 2111 (1975)]; K.D. Li and P.M. Fauchet, *Appl. Phys. Lett.* **51**, 1747 (1987).
- ²⁹ R. L. Fork, C. V. Shank, C. Hirlimann, R. Yen, and W. J. Tomlinson, *Opt. Lett.* **8**, 1 (1983).
- ³⁰ H. Schulz, J. Bialkowski, K. Sokolowski-Tinten, and D. von der Linde, in *Ultrafast Phenomena VII* (Ref. 12).
- ³¹ Reference 8 describes the observation of two different types of laser-induced phase transitions in *gallium arsenide*. Similar results have been obtained in *silicon* (unpublished).
- ³² M.L. Cohen and J.R. Chelikowski, in *Electronic Structure and Optical Properties of Semiconductors* (Springer, Berlin, 1989).
- ³³ K. Sokolowski-Tinten, J. Bialkowski, and D. von der Linde, in *Ultrafast Phenomena VIII*, edited by J.-L. Martin, A. Migus, G.A. Mourou, and A.H. Zewail, Springer Series in Chemical Physics Vol. 55 (Springer, Berlin, 1993).
- ³⁴ Y. Siegal, E.N. Glezer, and E. Mazur, *Phys. Rev. B* **49**, 16 403 (1994).
- ³⁵ *Handbook of Optical Constants of Solids*, edited by E. D. Palik, (Academic, Orlando, 1985).
- ³⁶ G. E. Jellison Jr., *Opt. Mater.* **1**, 41 (1992).
- ³⁷ N. Bloembergen, *Nonlinear Optics* (Benjamin, Reading, MA, 1982).
- ³⁸ J. Lekner, *Theory of Reflection* (Nijhoff, Dordrecht, 1987).
- ³⁹ W. Kütt, A. Esser, K. Seibert, U. Lemmer, and H. Kurz, in *Applications of Ultrashort Laser Pulses in Science and Technology* (Ref. 25), p. 154.
- ⁴⁰ D.H. Reitze, T.R. Zhang, Wm.M. Wood, and M.C. Downer, *J. Opt. Soc. Am. B* **7**, 84 (1990).
- ⁴¹ K. Sokolowski-Tinten, J. Bialkowski, and D. von der Linde (unpublished).
- ⁴² Equation (4) in Ref. 20 gives an explicit relation between the time required for the proposed transition to a new centrosymmetric but nonmetallic state of the solid phase and the strength of the optical excitation. This fluence-dependence is not consistent with our observation of a fluence independent time constant of the initial decay of $\chi^{(2)}$.
- ⁴³ See, for example, *Ultrafast Phenomena VIII*, (Ref. 33); or *Hot Carriers in Semiconductors VIII*, edited by J. E. Ryan and A. C. Maceil, special issue of *Semicond. Sci. Technol.* **9**, No. 5S (1994), and previous proceedings of these conferences.
- ⁴⁴ W.Z. Lin, R.W. Schoenlein, J.G. Fujimoto, and E.P. Ippen, *IEEE J. Quantum Electron* **24**, 267 (1988).
- ⁴⁵ T. Elsaesser, J. Shah, L. Rota, and P. Lugli, *Phys. Rev. Lett.* **66**, 1757 (1991).
- ⁴⁶ J.-L. Oudar, D. Hulin, A. Migus, A. Antonetti, and F. Alexandre, *Phys. Rev. Lett.* **55**, 2074 (1985).
- ⁴⁷ J. Shah, R.F. Leheny, and C. Lin, *Solid State Commun* **18**, 1035 (1976).
- ⁴⁸ P.A. Wolff, *Phys. Rev.* **126**, 405 (1962).
- ⁴⁹ R. Blank and H. Haug, *Phys. Rev. B* **44**, 10 513 (1991).
- ⁵⁰ R.A. Abram, G.N. Childs, and P.A. Saunderson, *J. Phys. C* **17**, 6105 (1984); A. Oschlies, R.W. Godby, and R.J. Needs, *Phys. Rev. B* **45**, 13 741 (1992).
- ⁵¹ P. Grosse, *Freie Elektronen in Festkörpern* (Springer, Berlin, 1979).
- ⁵² H.M. van Driel, *Appl. Phys. Lett.* **44**, 617 (1984).
- ⁵³ G.-Z. Yang and N. Bloembergen, *IEEE J. Quantum Electron.* **22**, 195 (1986).
- ⁵⁴ E.J. Yoffa, *Phys. Rev. B* **21**, 2415 (1980).
- ⁵⁵ M. Rasolt and H. Kurz, *Phys. Rev. Lett.* **54**, 722 (1985); M. Rasolt, *Phys. Rev. B* **33**, 1166 (1986).
- ⁵⁶ M. Combescot and J. Bok, *J. Lumin.* **30**, 1 (1985).
- ⁵⁷ M. Combescot and J. Bok, *Phys. Rev. Lett.* **51**, 519 (1983).
- ⁵⁸ C.V. Shank, R. Yen, and C. Hirlimann, *Phys. Rev. Lett.* **51**, 520 (1983).
- ⁵⁹ H. Kurz and N. Bloembergen, in *Energy Beam-Solid Interactions and Transient Thermal Processing, 1984*, edited by D. K. Biegelsen, G. A. Rozganyi, and C. V. Shank, MRS Symposia Proceedings No. 35 (Materials Research Society, Pittsburgh, 1985), p. 3.
- ⁶⁰ D. Hulin, M. Combescot, J. Bok, A. Migus, J.Y. Vinet, and A. Antonetti, *Phys. Rev. Lett.* **52**, 1998 (1984).
- ⁶¹ M. Combescot and R. Combescot, *Phys. Rev. B* **35**, 7986 (1987).
- ⁶² B.E. Sernelius, *Phys. Rev. B* **40**, 12 438 (1989); **43**, 7136 (1991).
- ⁶³ C.L. Tang and Chr. Flytzanis, *Phys. Rev. B* **4**, 2520 (1971).
- ⁶⁴ B.F. Levine, *Phys. Rev. Lett.* **22**, 787 (1969).
- ⁶⁵ R.K. Chang, J. Ducuing, and N. Bloembergen, *Phys. Rev. Lett.* **15**, 415 (1965).
- ⁶⁶ F.G. Parsons and R.K. Chang, *Opt. Commun.* **3**, 173 (1971).

- ⁶⁷ D. Bethune, A.J. Schmidt, and Y.R. Shen, Phys. Rev. B **11**, 3867 (1975).
- ⁶⁸ C.Y. Fong and Y.R. Shen, Phys. Rev. B **12**, 2325 (1975).
- ⁶⁹ D.J. Moss, J.E. Sipe, and H.M. van Driel, Phys. Rev. B **36**, 9708 (1987).
- ⁷⁰ N. Fabricius, P. Hermes, D. von der Linde, A. Pospieszczyk, and B. Stritzker, Solid State Commun. **58**, 239 (1986).